Growth of Crystalline Silicon for Solar Cells: Mono-Like Method

9

Kentaro Kutsukake

Contents

Abstract

The mono-like method, also known as the mono cast, seed cast, and quasi-mono methods, is a candidate next-generation method of casting Si ingots for solar cell applications, replacing conventional casting methods. The mono-like method provides single crystalline Si ingots with the use of almost the same facilities as those used for growth of multicrystalline Si ingots. Hence, the mono-like method has potential to achieve Si ingots with both high quality and low cost. However, the mono-like method faces challenges owing to its crystal growth processes,

K. Kutsukake (✉)
Center for Advanced Intelligence Project, RIKEN, Tokyo, Japan
e-mail: kentaro.kutsukake@riken.jp

D. Yang (ed.), *Handbook of Photovoltaic Silicon*,
https://doi.org/10.1007/978-3-662-56472-1_35

such as multicrystallization, dislocation generation, and impurity contamination. To address these problems, advanced mono-like methods have been developed. In this chapter, advanced mono-like methods are reviewed from the viewpoint of crystal growth and the fundamentals of the mono-like method.

Keywords
Silicon · Crystal growth · Mono-like · Seed growth · Seed cast · Quasi-mono · Dislocations · Dislocation generation · Grain boundaries · Defect engineering · Artificial grain boundaries · Functional defects

Introduction

The mono-like method is a growth method for single crystalline Si ingots based on a casting method. Almost the same growth furnace and procedures as those for multicrystalline silicon (mc-Si) can be used. The similarity with the mc-Si casting process leads to advantages in terms of low cost and high throughput. The main difference with mc-Si processes is that single crystalline Si ingots can be obtained with the use of single crystalline seeds. Generally, single crystalline Si solar cells show higher performance than those based on mc-Si, and this is also true for single crystalline Si grown by the mono-like method (e.g., Mrcarica 2013, Jay et al. 2014, and Jouini 2018). Thus, mono-like Si has both the advantages of single crystalline and multicrystalline Si and represents a potential high-quality low cost-material for solar cells.

The development of mono-like methods for solar cell applications started following the BP solar report (Stoddard et al. 2008). The idea of growing single crystalline Si in a crucible together with seed crystals had been suggested for a long time (e.g., Ciszek et al. 1979). The BP solar breakthrough was to demonstrate that a single crystalline ingot could be obtained with a practically useful size. Considerable research and development followed this initial report; however, the market share of the mono-like method remains low at present. The reasons for this low-market share are related to the ingot cost and quality, which are in turn controlled by the crystal growth process and crystal defects in mono-like ingots. Thus, further research to address these issues is necessary for developing and practically applying the mono-like method.

In this chapter, first the fundamentals of the mono-like method are described from the viewpoint of crystal growth. Then, advanced mono-like methods such as functional grain boundaries, functional defects, and mushroom-type interface growth are presented. Most of these advanced methods aim to control the generation and propagation of crystal defects during the crystal growth processes. Finally, future developments of the mono-like method are discussed.

Note that the growth method and single crystalline Si ingots grown in a crucible by the casting method are also described by the terms as seed cast, mono cast, and quasi-mono. In this chapter, the term “mono-like” is used collectively.

Fundamentals of the Mono-Like Method

Seed Growth

The Czochralski (CZ) method is well known for growingsingle bulk crystals by drawing seed crystals over the Si melt (see ▶ Chap. 6, "Growth of Crystalline Silicon for Solar Cells: Czochralski Si"). Seed crystals are also used directly inside the crucible in the Bridgman method. Figure 1 shows a schematic illustration of the vertical Bridgeman method. In the method, crystal growth is performed by slowly pulling the crucible down in a temperature gradient formed by separated heaters in the furnace. The crystal directionally grows from the melt as the materials move across the position corresponding to the melting point. In this process, if a seed crystal is placed at the bottom of the crucible, crystals with the same crystal orientation as the seed grow on the seed epitaxially. The mono-like method to produce single crystalline Si ingots for solar cells is basically same as the vertical Bridgman method in terms of the following technical features: it involves directional growth in a crucible from the bottom to the top and the use of single crystalline seeds.

From another point of view, the mono-like method is similar to the casting method used to produce mc-Si for solar cells (see ▶ Chaps. 8, "Growth of Multicrystalline Silicon for Solar Cells: Dendritic Cast Method," and ▶ 7, "Growth of Multicrystalline Silicon for Solar Cells: The High-Performance Casting Method"). Figures 2 and 3 show schematic illustrations of the casting method and mono-like method, respectively. In the case of the casting method, first, all the Si raw materials in a crucible are completely melted at a high temperature above the melting point. Then, the furnace is cooled down, and crystals grow directionally from the bottom to the top of the crucible. At the initial stage of this process, crystal grains randomly nucleate on the bottom surface of the crucible with various crystal orientations. These initial crystal grains act as a template for the following directional growth. As

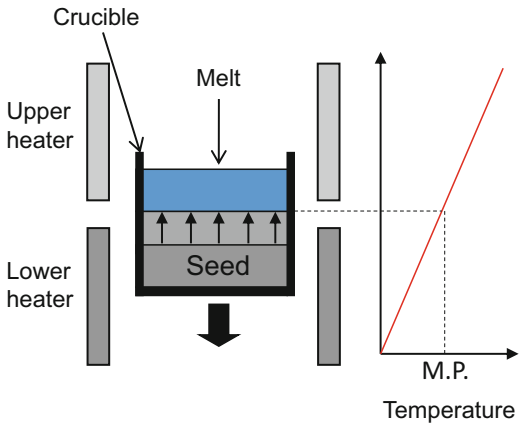

Fig. 1 Schematic illustration of vertical Bridgeman method

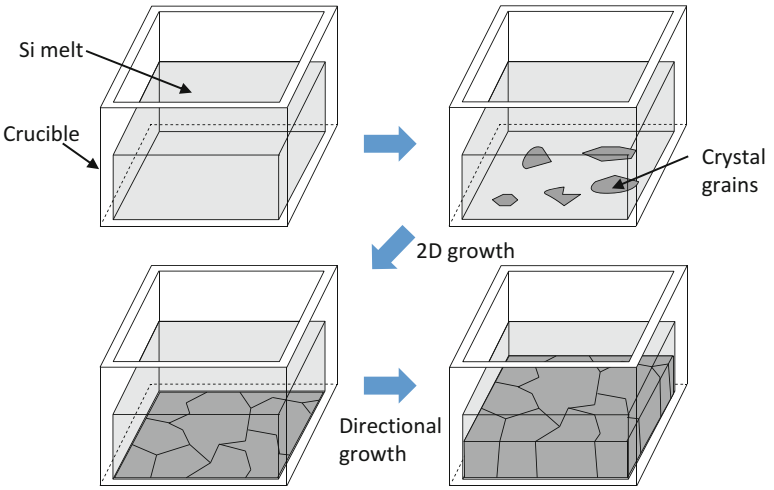

Fig. 2 Schematic illustration of mc-Si growth of the casting method

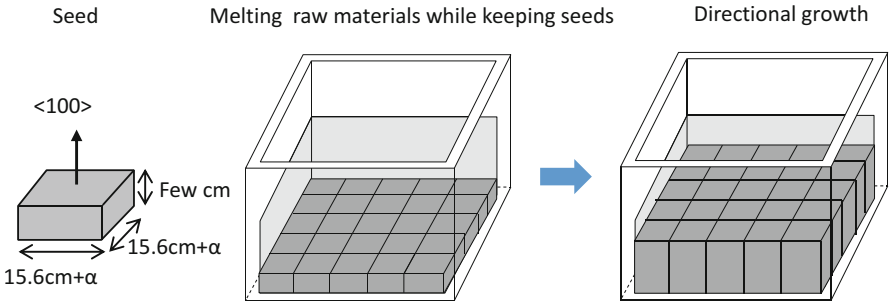

Fig. 3 Schematic illustration of seed and single crystalline growth of the mono-like method

a result, the grown ingot becomes a columnar multicrystal and inherits the initial grain structure.

However, in the case of the mono-like method, single crystalline seeds are used as a template for directional growth. Generally, the <100> orientation is selected for the crystal orientation of the seed in the growth direction in consideration of solar cell applications. These seed bricks are prepared from single crystalline CZ ingots. In the practical mono-like method, a typical seed size is similar to the size of solar cell wafers, i.e., $(15.6 + \alpha) \times (15.6 + \alpha) \times$ few cm^3. Here, α is the kerf for cutting ingots to bricks. For example, in the case of the growth of G5 size mono-like ingots, $5 \times 5 = 25$ seed bricks are needed as shown in Fig. 3. As in this example, multiple seed crystals are required for practical mono-like growth because a large seed crystal covering the whole area of the bottom of the crucible cannot be made from CZ ingots. Thus, boundaries between seed crystals are introduced into the ingot. These seed joints are a source of dislocation generation during crystal growth. This

problem will be discussed in the next section together with the other problems associated with the mono-like method. Except for the seed crystals, the same materials as the growth of mc-Si ingots can be used for the crucible, its coating, the Si raw materials, and flow gases.

For the ingot growth, a mc-Si crystal growth furnace can be used. In the growth procedure, to keeping the seed crystals solid during the melting process of the Si raw materials, the processing conditions and temperature profile require some modifications from those used to grow mc-Si ingots. These modifications lead to a slight increase of the processing time, typically less than few hours. There are almost no differences in the following growth processes: directional solidification, and cooling.

In the cutting process from ingots to bricks and the slicing process from bricks to wafers, almost the same facilities and sequences used for mc-Si can be applied to mono-like ingots (see ▶ Chap. 11, "Wafer Processing"). Additionally, for slicing, multiwire sawing using fixed diamond abrasive grains is applicable. This is a considerable advantage of the mono-like method and will be explained in the next section.

Advantages and Disadvantages of the Mono-Like Method

As described in the above section, the production facilities and processes for the mono-like method are similar to those used in the casting method for growth of mc-Si ingots. Therefore, the mono-like method has almost the same advantages as the casting method in terms of ingot production. Namely, it provides a high production throughput owing to the huge size of the ingots and the greater material yield owing to the square shape of ingots, comparing with the CZ method. Furthermore, mono-like and casting growth can be conducted with automatic operation; however, the CZ method needs human checking of the process when the seed touches the Si melt surface. These processing features reduce the production costs. Furthermore, the similarity with the casting method also lowers the barrier to introducing this method on a practical manufacturing line. Existing facilities for producing mc-Si ingots can also be effectively used for mono-like ingots.

Mono-like Si also has advantages in terms of its crystal quality. Mono-like Si ingots are single crystalline although these are sometimes termed "single-crystal-like" or "quasi-crystalline." Mono-like Si wafers share many of the advantages of single crystalline wafers made from CZ ingots. In mono-like Si wafers, there are no grain boundaries which operate as recombination sites for photogenerated carriers. Therefore, the conversion efficiency of solar cells based on mono-like Si wafers is potentially higher than that of mc-Si wafers containing electrically active grain boundaries.

Another advantage of single crystals is the uniform {100} crystal orientation of the wafer surface, which is beneficial for surface texturing in alkaline solution. This feature also contributes to better optical confinement by texturing and can be adapted to cost-effective multiwire sawing by fixed diamond abrasive grains. In the case of mc-Si, surface texturing is generally performed in acid solution owing to the

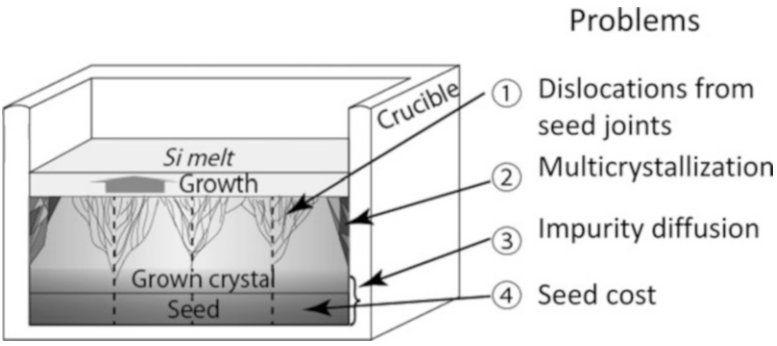

Fig. 4 Schematic illustration of the problems associated with the mono-like method

random crystal orientation of the wafer surface. Such acid texturing requires the formation of a surface damage layer formed by multiwire sawing with loose grains. However, multiwire sawing by fixed diamond abrasive grains forms a layer with little damage present. For these reasons, it is difficult to adapt cost-effective multiwire sawing by fixed-diamond abrasives to mc-Si. However, texturing of the {100} surface of single-crystalline Si in alkaline solution does not need a surface damage layer; therefore, mono-like Si is suitable for multiwire sawing by fixed-diamond abrasives.

As discussed above, mono-like Si shares many of the advantages of CZ-Si and mc-Si; however, these advantages can become limitations in certain cases. The crystal quality of mono-like Si is slightly worse than that of CZ-Si and mono-like Si has a slightly higher cost than that of mc-Si.

These crystal quality and cost issues are mainly related to the problems of growing crystals of mono-like Si ingots, as shown in Fig. 4. (1) Dislocation generation: a large number of dislocations are generated from grain boundaries formed at seed-crystal joints. These dislocations form clusters, which degrade solar cell performance. (2) Multicrystallization: crystal grains nucleate at the inner side walls of the crucible during directional crystal growth in the same way that grains nucleate on mc-Si at the bottom surface of the crucible. These crystal grains extend inside the ingot with directional growth. As a result, the obtained wafers become partially multicrystalline. (3) Impurity diffusion: the periphery region of an mc-Si ingot, a so-called red zone, typically shows low carrier lifetimes owing to solid phase diffusion of metallic impurities, such as iron, from the crucible and its coating materials. In the case of the mono-like method, the seed crystals remain solid in the high-temperature process of melting the raw materials. During the process, metallic impurities diffuse into the seed crystals from the bottom of the crucible. This diffusion results in a thicker bottom red zone for mono-like Si ingots than that of mc-Si ingots. (4) Seed cost: single crystalline seeds are made from CZ-Si ingots. This raises the cost of mono-like Si because, of course, CZ-Si is more expensive than the Si raw materials.

All these disadvantages are related to the crystal growth of mono-like Si, although each factor has a different influence. Thus, further fundamental studies of the crystal growth of mono-like crystals are needed. Investigations have been performed to try to resolve the issues related to the mono-like method. In the following sections, the mechanism of dislocation generation is discussed and advanced mono-like methods are described.

Dislocation Generation

As described in the above section, dislocations generated from grain boundaries formed by seed joints are a serious problem in mono-like Si. The problem of dislocation generation at grain boundaries is also common in the growth of mc-Si ingots (see ▶ Chaps. 18, "Defects in Crystalline Silicon: Dislocations," and ▶ 19, "Grain Boundaries in Multicrystalline Silicon"). Thus, many studies have been conducted to reveal the mechanism of dislocation generation during ingot growth. The studies can be roughly categorized into two types of investigations from different viewpoints: the influence of the grain boundary microstructure and the influence of the stress distribution. This section reviews studies on the mechanism of dislocation generation from grain boundaries from these two viewpoints.

Influence of Grain Boundary Microstructure

Grain boundaries can be categorized into three types by their misorientation angle, θ_R, as illustrated in Fig. 5. Grain boundaries with θ_R less than or equal to the critical angle, θ_C, are categorized as small angle boundaries (sub-grain boundary). The microstructure of small angle boundaries is described by aligned dislocations, as shown in Fig. 6. The distance between adjacent dislocations is inversely proportional

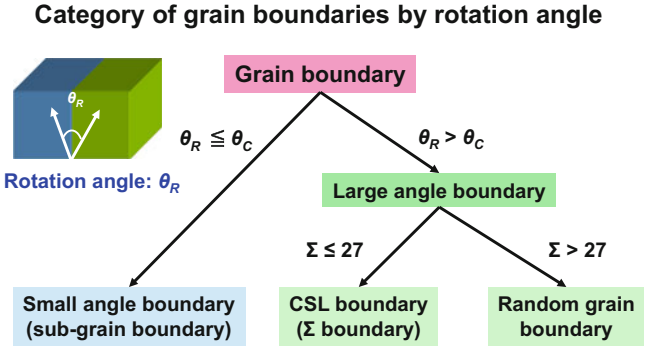

Fig. 5 Categories of grain boundaries based on rotation angle, where θ_C is the critical angle and **Σ** is determined by coincidence site lattice theory

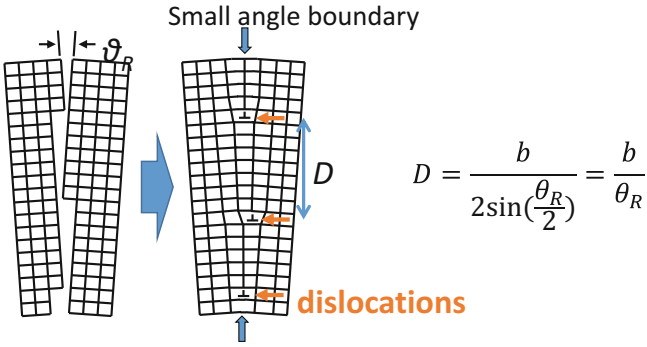

Fig. 6 Schematic illustration of the microstructure of small angle boundaries. In the equation, b is the length of the Burgers vector of the dislocations

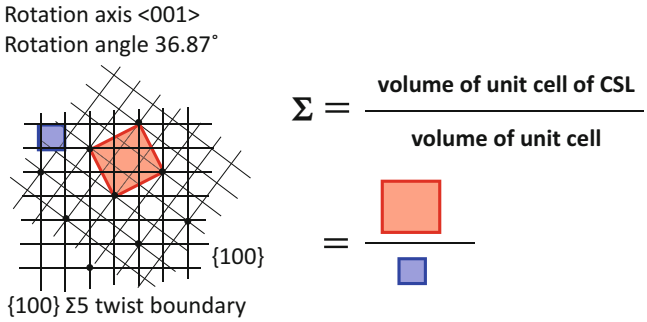

Fig. 7 Schematic illustration of the calculation of the **Σ** value. The displayed grain boundary is a {100} Σ5 twist boundary for a simple cubic lattice. The value of **Σ** is defined by the volume ratio of the unit cell of the CSL and volume of the unit cell

to θ_R. The type of dislocations introduced at the boundary plane depends on the component of θ_R: edge dislocations and screw dislocations are introduced to relax tilt and twist components of θ_R, respectively. Thus, the microstructure of small angle boundaries changes markedly with the angle and component of θ_R. The critical angle between small and large angle boundaries, θ_C, approximately corresponds to the angle at which the microstructure of the grain boundaries changes from that consisting of aligned dislocations to a random structure. In the case of Si crystals, an angle in the range of 10° to 15° is typically expected for θ_C.

Grain boundaries with θ_R larger than θ_C are considered to be large angle boundaries and these can be further divided into two groups based on their **Σ** value, which is determined by coincidence site lattice (CSL) theory (see Fig. 7). The **Σ** value shows the coherency of the two crystal lattices at both sides of the grain boundary. A smaller **Σ** value indicates a higher density of coincidence lattice points at the grain boundary surface, i.e., a more stable grain boundary structure. In the case of Si, large angle boundaries with **Σ** values less than or equal to 27 are considered to be CSL

boundaries, and other large angle boundaries with Σ values greater than 27 are considered to be random grain boundaries.

Deviation from the misorientation angle of a perfect CSL boundary is relaxed by insertion of grain boundary dislocations at the grain boundary plane, as for the case of small angle boundaries. Thus, the microstructures of CSL boundary are sensitive to change in the misorientation angle and its components. However, the microstructure of random grain boundaries is insensitive to small changes in the misorientation angle and its components. For these reasons, the influence of the grain boundary microstructure on dislocation generation is crucial for small angle and CSL boundaries in terms of the deviation angle from the perfect crystal and the perfect CSL misorientation, respectively. Experimentally, Wu et al. showed that a 0°-tilt boundary (note that in this paper there was no definition of small misorientation angle) generates dislocations more easily than large-angle tilt boundaries during the growth of mono-like Si ingots (Wu et al. 2016). Their results also support the above idea that dislocation generation from a small angle boundary is more sensitive to the microstructure than that from large angle random grain boundaries.

The influence of the misorientation angle of a small angle boundary on the dislocation generation was investigated in a mono-like Si ingot with <110> crystal orientations in the growth direction (Ekstrøm et al. 2015). They formed nine small angle boundaries in an ingot with boundary planes of {100}/{100} or {110}/{110} having different misorientations less than 0.6° using designed seed crystals. The dislocation generation from the boundaries was evaluated through photoluminescence imaging of horizontal cross sections of the ingot, as shown in Fig. 8. In the junctions containing no or small gaps, the amount of generated dislocations mainly depends on the misorientation between the adjacent seeds. High bulk lifetimes are retained for sufficiently low misorientations.

The gap between adjacent seeds is another parameter that determines the microstructure of grain boundaries formed by seed joints. Dislocation generation inside and above seed gaps during the growth of mono-like ingots has also been investigated (Trempa et al. 2014), by testing the influence of various parameters of the seeds joints, including: crystal orientation in the growth direction, crystal orientation of the gap plane, surface treatment of the gap surface, and the space of the gaps. Dislocations generated above the gaps were smaller for the <100> growth direction than those for the <110> and < 111> directions.

Influence of Stress Distribution

As described above, dislocation generation from a random grain boundary is insensitive to the microstructure. Thus, in the case of random grain boundaries, the influence of stress around the boundary has a greater influence on dislocation generation. Si crystals have an anisotropic elastic constant. Therefore, the macroscopic stress distribution in an ingot during the crystal growth process depends on the combination of crystal orientation of grains at both sides of the grain boundary as well as growth conditions, such as the temperature distribution and cooling speed.

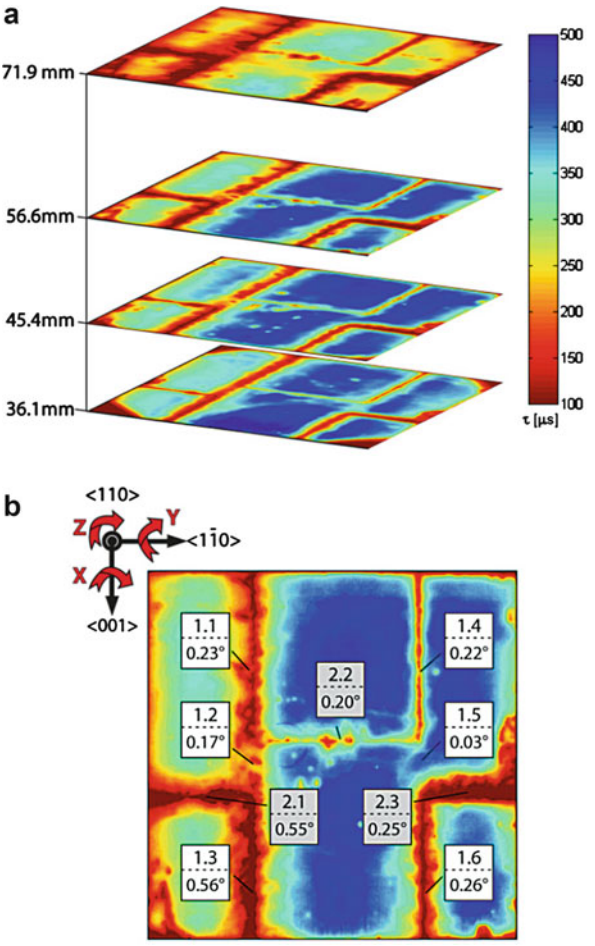

Fig. 8 (**a**) Carrier lifetime distribution evaluated by quantitative photoluminescence imaging. Junctions from 1.1 to 1.6 and from 2.1 and 2.3 in (**b**) are {110}/{110} and {100}/{100} junctions, respectively. The angle of each junction shows the misorientation angle of the boundaries. (From Ekstrøm et al. 2015)

The distribution of shear stress produced by isotropic deformation was calculated for various combinations of crystal grain orientation grains by a finite element method and the calculation results were compared with experimental results for the growth of small mono-like ingots (Takahashi et al. 2010). The amount of observed dislocations generated from a random grain boundary showed a positive correlation with the magnitude of the numerically calculated shear stress, as calculated for the crystal orientations of the grain boundary.

The dislocation behavior in mono-like Si with a seed junction and single crystalline Si without a seed junction has been investigated from the view point of the stress distribution during crystal growth processes (Jiptner et al. 2016). Single crystalline Si results have shown that dislocation motion has a considerable influence on the dislocation distribution in the (111) system. Long slip lines were observed in (111)-oriented ingots but not in (100)-oriented ingots. Experimental results and

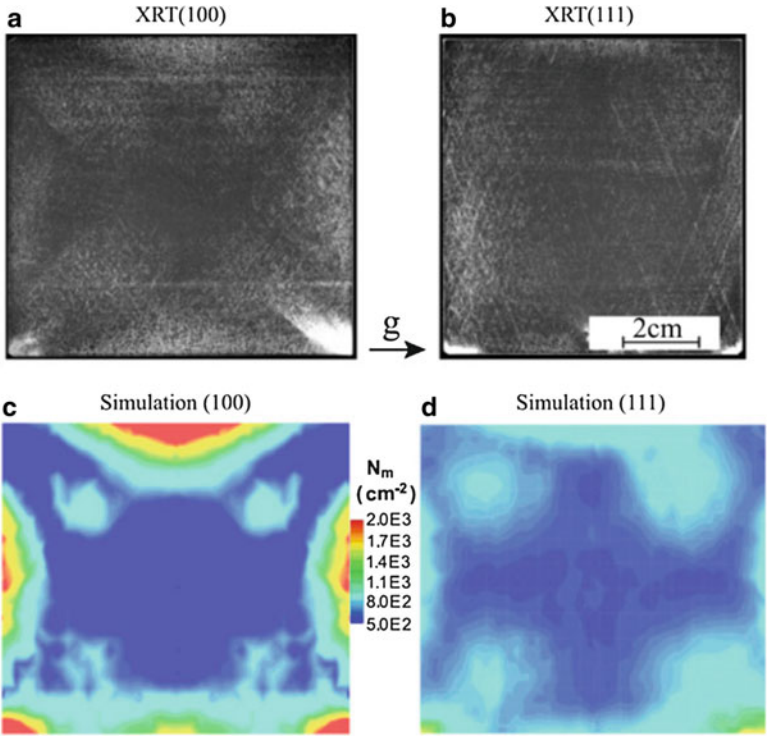

Fig. 9 X-ray topography images of (**a**) <100> and (**b**) <111> single crystalline Si ingots after annealing experiments and the distribution of dislocation density of (**c**) <100> and (**d**) <111> ingots predicted by numerical simulation. (From Jiptner et al. 2016)

numerical simulations using the Hasen–Alexander–Sumino model showed good correlation; however, simulations cannot correctly predict such long dislocation motion, as shown in Fig. 9.

Advanced Mono-Like Methods

Functional Grain Boundaries

Generally, grain boundaries have anegative impact on solar cell performance, acting as carrier recombination sites and a source of dislocations. In the early 2000s, the concept of controlling multicrystalline structures was proposed by Nakajima's group (see Fig. 1 in ▶ Chap. 8, "Growth of Multicrystalline Silicon for Solar Cells: Dendritic Cast Method"). An ideal grain boundary is described as electrically inactive with the ability to act as a sink for other defects, such as point defects, impurities, and dislocations. Thus, the positive features of grain boundaries can be used to improve solar cell performance.

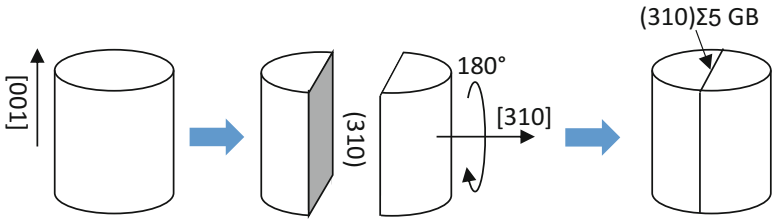

Fig. 10 Seed design for forming a {310}Σ5 grain boundary

The idea of a functional grain boundary was conceived based on the above concept (Kutsukake et al. 2013). Furthermore, in addition to the taking advantage of the positive features of grain boundaries, the idea of controlling grain boundary structures in multi-seed crystals has been adapted.

The growth of artificial grain boundaries in bulk Si crystals based on multi-seed crystals has been developed to investigate microstructure, growth phenomena, and electrical properties of the grain boundaries, before the BP solar report on mono-like Si in 2008. In particular, coincidence site lattice (CSL) grain boundaries have been well investigated, including: {111}Σ3 and {221}Σ9 grain boundaries grown by the CZ method (Endrös 2002); {111}Σ3 grain boundaries grown by floating zone (FZ) method (Kitamura et al. 2005); {310}Σ5 grain boundaries grown by the vertical Bridgeman method (Kutsukake et al. 2007a); {310}Σ5 grain boundaries grown by the FZ method (Kutsukake et al. 2007b); and random grain boundaries grown by the CZ method (Hoshikawa et al. 2007). Among the various CSL boundaries, Σ5 grain boundaries are notable as potential functional grain boundary candidates because they have the lowest sigma value in the CSL grain boundary family parallel to the <100> crystal orientation, which is a useful orientation for solar cell applications. Figure 10 shows the seed design for forming a {310}Σ5 grain boundary grown by the vertical Bridgman method. A columnar single crystalline Si with a [001] crystal orientation in the growth direction was cut along the (310) plane perpendicular to the growth direction. Then, one crystal piece was rotated 180° around the [310] axis perpendicular to the cutting plane. Through this operation, a Σ5 relationship was formed between the two crystal pieces. A {310}Σ5 grain boundary can be artificially formed by epitaxial growth on these multi-seed crystals in the vertical Bridgeman method.

The {310}Σ5 grain boundaries formed by such designed multi-seed crystals have been used as functional grain boundaries to suppress multicrystallization, which is a crystal growth issue associated with the mono-like method, as mentioned in the previous section. Figure 11 shows a schematic illustration and photographs of vertical cross sections of mono-like Si ingots with and without functional grain boundaries to suppress multicrystallization (Kutsukake et al. 2014). The ingot without functional grain boundaries corresponds to a conventional mono-like Si ingot.

During directional growth of mono-like Si ingots, {111}Σ3 grain boundaries frequently form at the crucible side walls accompanied by nucleation of multi-crystalline grains. The {111} grain boundary plane of the formed {111}Σ3 grain

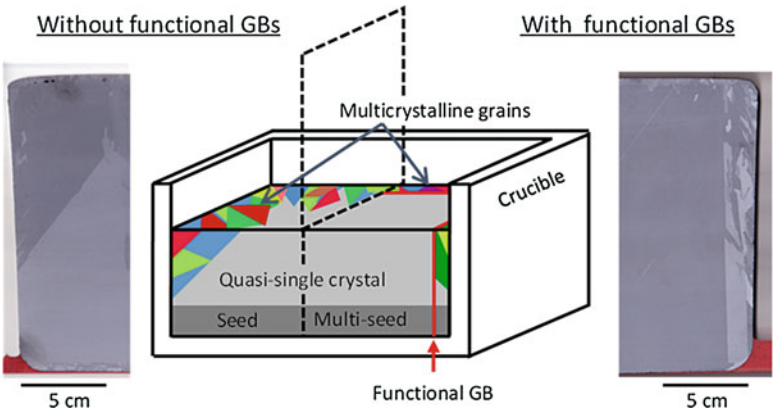

Fig. 11 Schematic illustration and photographs of vertical cross sections of mono-like Si ingots with and without functional grain boundaries to suppress multicrystallization

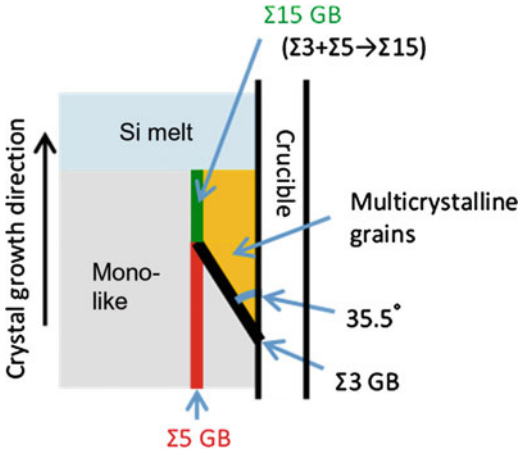

Fig. 12 Schematic illustration of the mechanism by which multicrystallization is suppressed

boundaries inclines from the [001] crystal orientation in the growth direction of the mono-like ingots. The area of multicrystalline grains consequently increases with the crystal growth direction. As a result, conventional mono-like wafers along the crucible side walls contain a large multicrystalline area.

In the case of a mono-like Si ingot with functional grain boundaries, {310}Σ5 grain boundaries form near the crucible side walls for multi-seed crystals. Figure 12 shows a schematic illustration of the mechanism by which multicrystallization is suppressed. The {310}Σ5 grain boundaries have a stable configuration in the [001] crystal orientation, and therefore extend straight in the growth direction of the mono-like Si ingot. The {111}Σ3 grain boundaries formed on the crucible side walls were converted into {310}Σ15 grain boundaries by interaction with {310}Σ5 grain boundaries. The {310}Σ15 grain boundaries have a stable configuration in the [001] crystal orientation, and therefore extend straight in the growth direction of

the mono-like Si ingot as {310}Σ5 grain boundaries. As a result, extension of multicrystalline grains inside the ingot was prevented and the multicrystalline regions were confined to the periphery of the ingot. As mentioned in the previous section, such periphery regions correspond to the red zone, which is a highly contaminated area and not used for solar cell wafers. Therefore, the material yield is not impaired by the functional grain boundary method.

Moreover, the functional grain boundary method also has the advantage of a wide processing window. The grain boundary interaction is determined only by the crystallographic geometry and does not depend on the crystal growth conditions, such as growth rate, magnitude of the temperature gradient, and crystal size. Therefore, multicrystallization of mono-like Si can be suppressed by replacing conventional seeds with functional grain boundary seeds without changing growth conditions.

Seed Manipulation for Artificially Controlled Defects Technique (SMART)

Takahashi et al. extended the idea of functional grain boundaries to functional defects and proposed the seed manipulation for artificially controlled defects technique (SMART). Figure 13 shows a schematic illustration of SMART. This method used two types of functional grain boundaries to generate dislocations and block dislocation propagation. Dislocations make positive contributions to impurity gettering and stress relaxation with plastic deformation in the crystal growth process; however, dislocations also have considerable negative effects, acting as carrier recombination sites in solar cell wafers. To take advantage of their positive effects, dislocations are intentionally and locally introduced as functional defects in functional grain boundaries formed from multiple seed crystals. However, introduced dislocations normally propagate to a large area in the ingot with directional growth

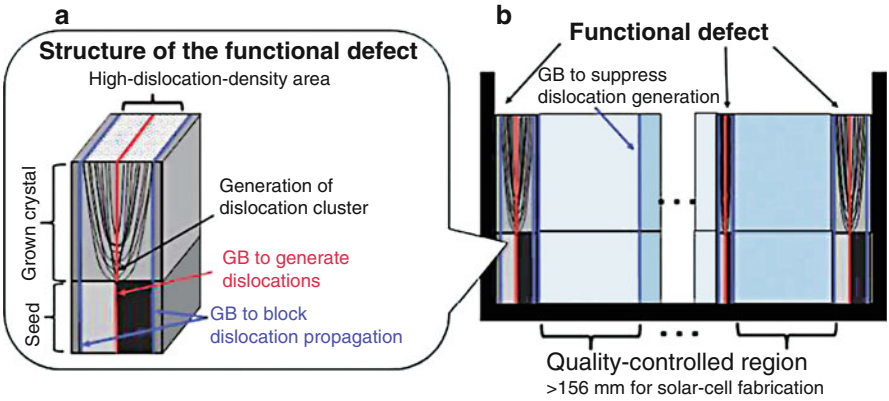

Fig. 13 Concept of SMART. (**a**) Structure of functional defects and (**b**) arrangement of seeds and grown crystals in a crucible. (From Takahashi et al. 2015)

as in the case of dislocations generated at seed joints. Thus, to block propagation of the dislocations, another type of functional grain boundary is also formed along the functional grain boundary used to generate dislocations. As a result, a high-density group of dislocations is confined in a thin region of the ingot. In addition, it is possible to make functional grain boundaries with the ability to both block propagation of dislocations and extension of multicrystalline grains. Therefore, by controlling the configuration of these thin dislocation regions overlapping with the ingot portion not used for solar cells, i.e., the red zones and cutting kerfs, high-quality ingots with a high yield ratio are achieved.

The effectiveness of SMART has been demonstrated through growth of laboratory scale ingots. Figure 14 shows a crystal orientation image map and an etch pit image of the vertical cross section of an ingot grown by SMART. Functional grain boundaries having the ability to generate dislocations were formed at the periphery of the ingot along the crucible side walls accompanied by those having the ability to block dislocation propagation inside them. In addition, at the center of the ingot, a grain boundary was formed as a model of that which forms at a seed joint. The etch pit image clearly shows that propagation of the dislocations generated by the functional grain boundaries was blocked by other functional grain boundaries. Inside the

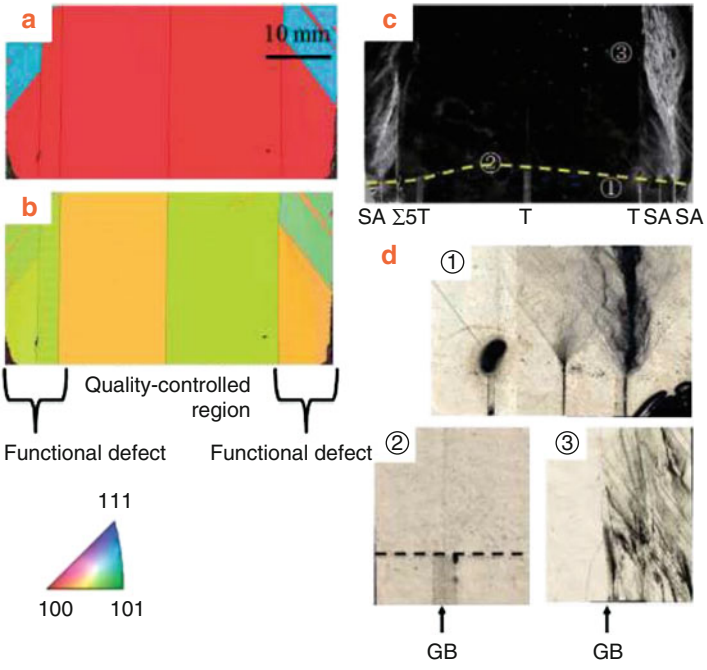

Fig. 14 (**a**) Orientation maps of growth direction, (**b**) the GB plane, (**c**) an etch pit image, and (**d**) magnified images taken by an optical microscope. In the orientation maps, the GBs – except for the SA GB – are separated by lines. The number in (**d**) corresponds to the observed area in (**c**). The dashed lines show the interface between the unmelted seeds and grown crystals. (From Takahashi et al. 2015)

functional grain boundaries, there were no clear etch pits from dislocation clusters. In particular, no dislocation clusters were generated at the grain boundary in the center of the ingot. This result suggests that dislocations intentionally introduced contribute to reduced stress during the thermal process of the crystal growth. Thus, the dislocations acted as functional defects.

Control of Seed Joint Structure: Special Grain Boundaries and Seed Partitions

Suppression of dislocation generation from grain boundaries formed at seed joints is a serious issue for mono-like Si. Dislocation generation from grain boundaries also affects the growth of mc-Si. Therefore, a number of studies have examined the mechanism of dislocation generation, as discussed in the previous section. In this chapter, two methods of using seed joint structures are addressed as candidates for next-generation mono-like methods.

Hu et al. reported the growth of high-quality mono-like Si withspecial grain boundaries (Hu et al. 2015). Two 870 × 870 × 300 mm^3 ingots were grown. One conventional (100)-oriented mono-like Si with small-angle grain boundaries at the seed joints. The other with special grain boundaries between the adjacent (100)-oriented seed crystals with a twisted angular deviation of 10°–45°. Figure 15 shows photoluminescence images of the wafers (a1–3) with small-angle grain boundaries

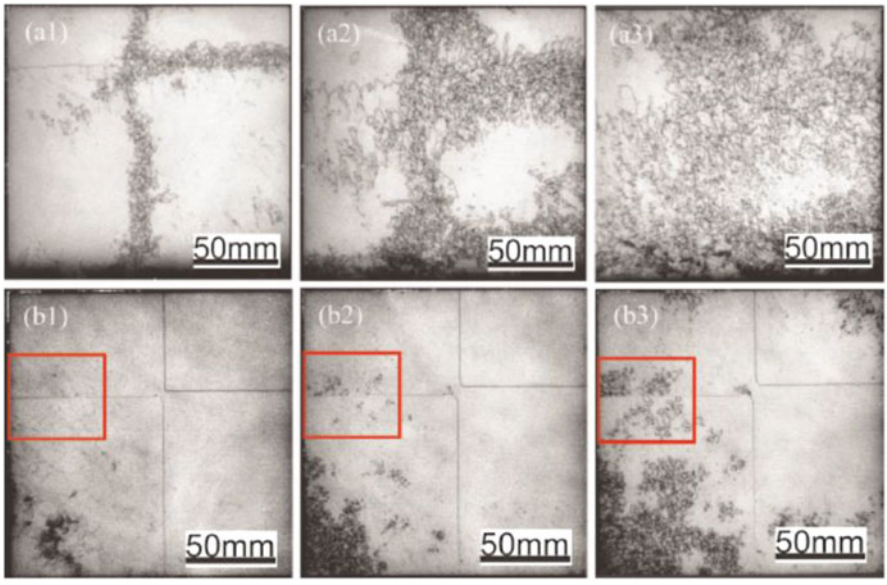

Fig. 15 Photoluminescence images of the wafers from the bottom (a1,b1), middle (a2,b2), and top (a3,b3) of the block of (**a**) ingot with small angle grain boundaries and (**b**) ingot with special grain boundaries. (From Hu et al. 2015)

and (b1–3) shows that with the special grain boundaries. Considerably fewer dislocation clusters were generated from the special grain boundaries than those from the small angle grain boundaries. As a result, the average conversion efficiency of the solar cells was reported to be 18.1%, which is 0.6% higher than the efficiency of conventional cells. Although these results are promising, the details of the seed orientation and configuration have not been disclosed.

Lan et al. proposed a simple approach usingseed partitions (Lan et al. 2017). Between the seed crystals with the same crystal orientation, thin Si plate seeds with a 30° or − 30° tilt angle from both sides of the seed crystals were inserted. As a result, two parallel grain boundaries with 30° or − 30° tilt angles were formed at both sides of the thin seed crystals in the grown mono-like Si ingot. Etch pit observations showed that these grain boundaries effectively suppressed dislocation generation. Furthermore, two advantages are emphasized: the ease of seed preparation and the lack of color mismatch. By this method, the main seed crystals have the same three-dimensional crystal orientation. Therefore, the seed preparation is much easier than that for combination seeds with special crystal orientations. Moreover, the same crystal orientation mitigates mismatch of the color of the solar cell surface, which appears after application of an anti-reflection coating, as shown in Fig. 16.

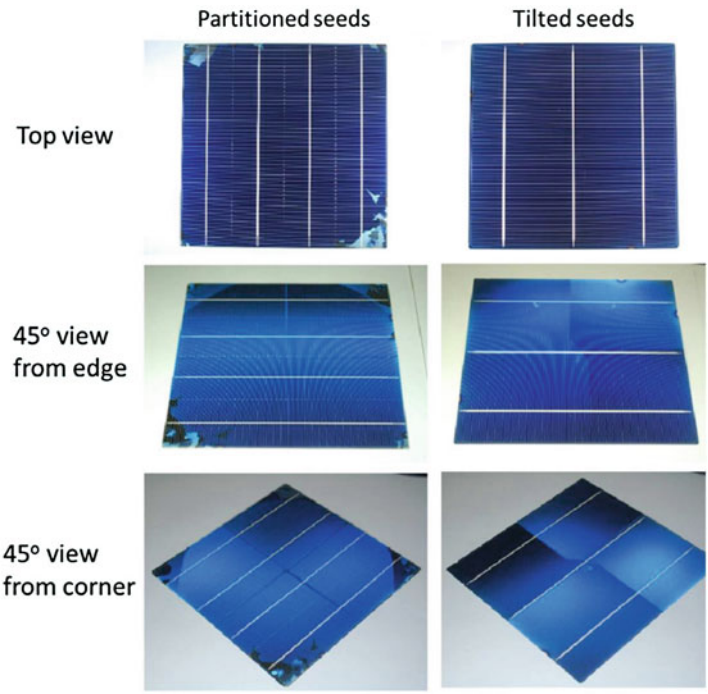

Fig. 16 Appearances at different view angles for the solar cells made from: (**a**) partitioned seeds; (**b**) tilted seeds. (From Lan et al. 2017)

Mono-Like Growth Without Seed Joints: Large Seed and Mushroom-Type Interface Growth

Another idea to suppress dislocation generation from seed joints is simply to rid the seed crystals of dislocation sources, i.e., seed joints. Two methods have been proposed: the use of large seed crystals and growth from small seed crystals.

As mentioned previously, the typical size of a seed crystal is almost the same as that of a solar cell wafer, i.e., $(15.6 + \alpha) \times (15.6 + \alpha)$ cm^2. These seed crystals are prepared from slices perpendicular to the growth direction of the CZ ingots. Gu et al. used rectangular plates cut along the axial direction of CZ columnar ingots as seed crystals for mono-like Si (Gu et al. 2012). The seed crystals were prepared to have a $< 100>$ crystal orientation in the growth direction. Dislocation generation was successfully suppressed in the vertical cross-section of the ingot along the longitudinal direction of the rectangular seeds. However, in another cross-section perpendicular to the longitudinal direction of the rectangular seeds seed joints existed as in the case of seed joints from conventional mono-like ingots.

Zhang et al. also proposed the use oflarge rectangular seed crystals; however, they used the $<110>$ crystal orientation as the growth direction of the mono-like ingots (Zhang et al. 2018). They suggested that multiplication of dislocations in the ingot with the $<110>$ growth direction was milder than that with $<100>$ growth direction. Therefore, although the dislocation density at the bottom of the ingot was higher in the ingot with the $<110>$ growth direction than that with $<100>$ growth direction, the total dislocation density in the ingot was reduced by using $<110>$ seed crystals. Furthermore, for applications to solar cell wafers, square column bricks are cut along the $<100>$ crystal orientation, which is perpendicular to both the growth direction of the ingot and the longitudinal direction of the rectangular seeds.

Another idea to rid seed crystals of seed joints is to grow the ingot from one small seed crystal. Kakimoto's group developed this growth method, so-called mushroom-type interface growth. Numerical simulation modeling of the conditions inside the growth furnace revealed characteristics of the mushroom-type interface growth, as well as details of the thermal condition of the growth (Gao et al. 2012). On the basis of the results of this numerical study, the method was applied to growth of a 50-cm^2 mono-like ingot (Miyamura et al. 2014). By controlling the shape of the liquid-solid interface, a mono-like crystal was grown from a small seed 20 cm in diameter. A dislocation density of 3×10^4 cm^{-2} was achieved.

Conclusions

The mono-like method can provide single crystalline Si ingots using the same facilities currently used for production of mc-Si ingots. Thus, this method has advantages of mc-Si in terms of low cost and high production throughput, and the uniform crystal orientation and high crystalline quality of CZ-Si. However, current

mono-like Si is intermediate between mc-Si and CZ-Si in terms of crystalline quality and production cost. Many of the issues associated with crystalline quality are related to the crystal growth process of mono-like ingots, such as multi-crystallization, dislocation generation, and impurity contamination. To resolve these problems, advanced mono-like methods have been proposed based on fundamental studies of crystal growth and defect generation in mono-like Si. Control of crystal orientation and the configuration of the seed crystals show promise as methods for addressing the issues of crystallinity. This chapter reviews functional grain boundaries, SMART, special grain boundaries, seed partitions, large seeds, and one-small seed. In addition to these methods considerable research has been done to develop mono-like Si methods. Although these methods are promising, further investigations of mono-like Si will be necessary. For instance, in the near future, the average dislocation density will become a problem for super-high efficiency solar cell application. To address this issue, further studies on seed preparation and optimization of thermal process are needed.

Cross-References

- ▶ Defects in Crystalline Silicon: Dislocations
- ▶ Grain Boundaries in Multicrystalline Silicon
- ▶ Growth of Crystalline Silicon for Solar Cells: Czochralski Si
- ▶ Growth of Crystalline Silicon for Solar Cells: Noncontact Crucible Method
- ▶ Growth of Multicrystalline Silicon for Solar Cells: Dendritic Cast Method
- ▶ Growth of Multicrystalline Silicon for Solar Cells: The High-Performance Casting Method

Acknowledgment The author is very grateful to Professor Kazuo Nakajima from Tohoku University for fruitful discussions about the fundamentals of crystal growth and defects generation of mono-like Si.

References

M. Mrcarica, Photo-Dermatology **19**, 28 (2013)

F. Jay, D. Muñoz, T. Desrues, E. Pihan, V. Amaral de Oliveira, N. Enjalbert, A. Jouini, Solar Energ. Mater. Solar Cells **130**, 690 (2014)

A. Jouini, in *Abstract of the 10th International Workshop on Crystalline Silicon for Solar Cells (CSSC-10)* (2018), p. 9

N. Stoddard, B. Wu, L. Witting, M. Wagener, Y. Park, G. Rozgonyi, R. Clark, Solid State Phenom. **1**, 131–133 (2008)

T.F. Ciszek, G.H. Schwuttke, K.H. Yang, J. Cryst. Growth **46**, 527 (1979)

K.E. Ekstrøm, G. Stokkan, R. Søndenå, H. Dalaker, T. Lehmann, L. Arnberg, M. Di Sabation, Phys. Status Solidi A **212**, 2278 (2015)

Y.C. Wu, A. Lan, C.F. Yang, C.W. Hsu, C.M. Lu, A. Yang, C.W. Lan, Cryst. Growth Des. **16**, 6641 (2016)

M. Trempa, C. Reimann, J. Friedrich, G. Mueller, A. Krause, L. Sylla, T. Richter, J. Cryst. Growth **405**, 131 (2014)
I. Takahashi, N. Usami, K. Kutsukake, G. Stokkan, K. Morishita, K. Nakajima, J. Cryst. Growth **312**, 897 (2010)
K. Jiptner, Y. Miyamura, H. Harada, B. Gao, K. Kakimoto, T. Sekiguchi, Prog. Photovolt. Res. Appl. **24**, 1513 (2016)
K. Kutsukake, N. Usami, Y. Ohno, Y. Tokumoto, I. Yonenaga, Appl. Phys. Express **6**, 025505 (2013)
A.L. Endrös, Sol. Energ. Mater. Sol. Cells **72**, 109 (2002)
M. Kitamura, N. Usami, T. Sugawara, K. Kutsukake, K. Fujiwara, Y. Nose, T. Shishido, K. Nakajima, J. Cryst. Growth **280**, 419 (2005)
K. Kutsukake, N. Usami, K. Fujiwara, Y. Nose, K. Nakajima, J. Appl. Phys. **101**, 063509 (2007a)
K. Kutsukake, N. Usami, K. Fujiwara, Y. Nose, T. Sugawara, T. Shishido, K. Nakajima, Mater. Trans. **481**, 143 (2007b)
T. Hoshikawa, T. Taishi, X. Huang, S. Uda, M. Yamatani, K. Shirasawa, K. Hoshikawa, J. Cryst. Growth **307**, 466 (2007)
K. Kutsukake, N. Usami, Y. Ohno, Y. Tokumoto, I. Yonenaga, IEEE J. Photovolt. **4**, 84 (2014)
I. Takahashi, S. Joonwichien, T. Iwata, N. Usami, Appl. Phys. Express **8**, 105501 (2015)
D. Hu, S. Yuan, L. He, H. Chen, Y. Wan, X. Yu, D. Yang, Solar Energ. Mater Solar Cells **140**, 121 (2015)
C.Y. Lan, Y.C. Wu, A. Lan, C.F. Yang, C. Hsu, C.M. Lu, A. Yang, C.W. Lan, J. Cryst. Growth **475**, 136 (2017)
X. Gu, X. Yu, K. Guo, L. Chen, D. Wang, D. Yang, Solar Energ. Mater. Solar Cells **101**, 95 (2012)
F. Zhang, X. Yu, S. Yuan, L. He, H. Chen, R. Hu, and D. Yang, in *Abstract of the 10th International Workshop on Crystalline Silicon for Solar Cells (CSSC-10)* (2018), p. 19
B. Gao, S. Nakano, H. Harada, Y. Miyamura, T. Sekiguchi, K. Kakimoto, J. Cryst. Growth **352**, 47 (2012)
Y. Miyamura, H. Harada, K. Jiptner, J. Chen, R.R. Prakash, S. Nakano, B. Gao, K. Kakimoto, T. Sekiguchi, J. Cryst. Growth **401**, 133 (2014)